Chapter 13
Design of a Five DOF Contactless Robot for Facade Inspection

Ginna Marcela García-Rodríguez, Eduardo Castillo-Castañeda, and Med Amine Laribi

Abstract Service tasks on vertical surfaces such as building facades continue to be performed manually by specialized technicians operating from complex scaffolding. This way of performing these tasks, in addition to being inefficient, is costly and dangerous for personnel who must work under the risk of falls. The façade inspection task, as well as façade cleaning task, can be achieved by following zig-zag motions to cover the whole working surface while keeping the tool perpendicular to the façade surface. The aim of this work is to develop a robotic inspection device of 5 degrees of freedom based on a Cartesian configuration with three translations and a pan-tilt type system with two rotations. The robotic device will be placed in front of the façade of a building, which can be previously characterized by a cloud of points. The kinematics of the robots is also presented as well as the mechanical elements to build a scalable prototype that can be sized according to the building dimensions.

Keywords Service robot · Cartesian configuration · Façade inspection · Inspection trajectories

13.1 Introduction

The construction of increasingly tall buildings, technological advances, and the realization of mandatory periodic inspections of buildings, are factors that promote the development of practical and innovative systems that facilitate the execution of these tasks. The robotization of inspection tasks leads to the optimization of processes in relation to time and cost, reduction of operational risks, and minimization of affections around the target structure of the inspection. The use of climbing robots

G. M. García-Rodríguez · E. Castillo-Castañeda
Instituto Politécnico Nacional, CICATA-Unidad Querétaro, Santiago de Querétaro, Mexico
e-mail: ecastilloca@ipn.mx

M. A. Laribi (✉)
Université de Poitiers, Institut PPRIME—DMSC, Chasseneuil-du-Poitou, France
e-mail: med.amine.laribi@univ-poitiers.fr

© The Author(s), under exclusive license to Springer Nature Switzerland AG 2024
M. Ceccarelli and J. C. Jauregui-Correa (eds.), *State-of-the-Art and Innovations in Mechanism and Machine Science*, Mechanisms and Machine Science 150,
https://doi.org/10.1007/978-3-031-47040-0_13

designed for inspection, maintenance, and many other tasks related to the construction sector, has been acquiring great relevance in recent times. Service robotics is an area of great opportunity that, since 2019, has been the one with the greatest development and the one that has generated the greatest increase in sales. Cleaning and inspection tasks are part of service robotics; However, there are very few commercial robots that perform these tasks on vertical surfaces [1].

At first, the use of inspection robots was established for hazardous environments with serious risks to the health and integrity of human operators. Currently, the field of application of this type of robots is booming and not only for dangerous industrial actions, but also for other areas of inspection and maintenance such as: construction, the electrical sector, forestry, among others. The objective is none other than to facilitate the work of workers by minimizing risks, execution time, and costs [2]. The construction sector has produced in recent decades a remarkable increase in the development of very tall buildings and structural ensembles with peculiar architecture, which, under traditional techniques, make access to the operational surface of inspection and maintenance difficult, expensive, and dangerous [3].

The integration of autonomous robotic systems in these tasks on vertical surfaces is presented as a technological challenge itself, in relation to the support of the system on the surface, to its displacements along it, and even more important, to have an obstacle detection system, necessary for the definition of the trajectory.

Among the main robotic developments focused on inspection and cleaning, there are some works such as: robot with sliding guide integrated to the glass facades with suction cup adhesion driven by pneumatic actuators [4]; prototype with passive suction cup adhesion [5] and device that uses negative pressure between the robot and the wall through vacuum pumps to adhere to the surface [6]. There are also robots with magnetic grip for metallic tanks [7]. Rope or rail grip is another method where the robot is held from the wall or ceiling via a rope or cable, allowing mobility and safe execution of tasks [8]. Robots with bioinspired adhesion have also been proposed, with the ability to scale vertical walls even on uneven surfaces such as concrete [9]. However, the force of gravity and the irregularity of the surfaces (for materials other than glass) of the facades, have become a challenge to achieve the high levels of adaptability and flexibility required by climbing robots in the execution of vertical tasks. Most traditional inspection systems are limited to structures such as scaffolding, hanging platforms through cables, articulated arms, and lifting platforms.

Regarding autonomous systems, the drones that have acquired great importance and popularity in recent years in multisectoral tasks [10], mainly in inspection. However, limitations in legislation, payload and stability against external environmental agents, due to their operational exposure to the elements, are some of the challenges they have nowadays. Recognizing the interest of prof Carlos Lopez-Cajun in investigating on designs of Robots, but with special attention to new solutions, this contribution refers to his interest in parallel manipulators and cable driven systems.

The aim of this work is to develop a robotic inspection device of 5 degrees of freedom based on a Cartesian configuration with three translations and a pan-tilt type system with two rotations. The robotic device will be placed in front of the façade of a building, which can be previously characterized by a cloud of points.

(a) (b)

Fig. 13.1 Inspection of a façade: **a** traditional way, **b** ideal trajectory

13.2 Inspection Task for Building Facades

Traditionally, building inspection tasks are performed manually following zig-zag trajectories, the technician moves horizontally until he covers the total length of the building, then he performs a downward displacement and covers again the total length of the building [11], see Fig. 13.1a. This trajectory is made from top to bottom until it covers the entire height of the façade, see Fig. 13.1b.

From these basic inspection task motions, the fundamental requirements were obtained to select the mobility of the proposal presented in this paper. The first refers to its locomotion, which must have 3 GDL to efficiently cover the area to be inspected, that is, to provide adaptability to the surface (concavities and convexities) and maneuverability both horizontally and vertically. The second requirement is the positioning capacity of its end effector (for the present case, the inspection sensor), so that it should be perpendicular to any point of the vertical surface. For the first requirement, the simplest option to obtain three translations is the cartesian configuration. For the second, a pan-tilt system was selected for end effector orientation, where the inspection sensor, a pachometer, will be mounted to evaluate the condition of a façade.

13.3 Conceptual Design of the Proposal

Compared to other proposals of service robotics, where the robot climbs to the surface of the building, our concept consists of a robot located in front of the façade, without making direct contact with it, see Fig. 13.2.

To define the CAD model of the proposal, aspects such as: locomotion, adaptability to the surface, trajectories of the end effector, horizontal and vertical maneuverability, simplicity of assembly, weight and type of control were considered. The needs that the robot must cover are focused: on the reach to all points of the façade

Fig. 13.2 Full view of the conceptual design proposal

surface considering the different profiles (concavities and convexities); the monitoring of the determined inspection path; the range of orientations, positions, and velocities; the efficiency and effectiveness of the inspection task.

13.4 Forward and Inverse Kinematics

The kinematic analysis of the device is simplified considering that it is composed of two parts: a Cartesian configuration structure and a pan-tilt system. Figure 13.3 shows the diagram of the robot of 5 DOF: 3 translations and 2 rotations. The pose of the end effector is defined by Px, Py, Pz, ϕ, θ.

The corresponding Denavit-Hartenberg parameters are shown in Table 13.1.

The dimensions of the robot are defined by the constants a_1, a_2, a_3, a_4, a_5, a_6, Joint variables by translational distances d_1, d_2, d_3 and by angles θ_1, θ_2. The first three homogeneous transformation matrices corresponding to the three translations of the robot are shown in Fig. 13.4.

The last two homogeneous transformation matrices corresponding to the two rotations of the robot are shown in Fig. 13.5.

By multiplying the above transformation matrices, one can establish the closed-loop equation of the mechanism:

$$^{0}T_{N} = {}^{0}T_{1}\,{}^{1}T_{2}\,{}^{2}T_{N-1}\ldots{}^{N-1}T_{N} \tag{13.1}$$

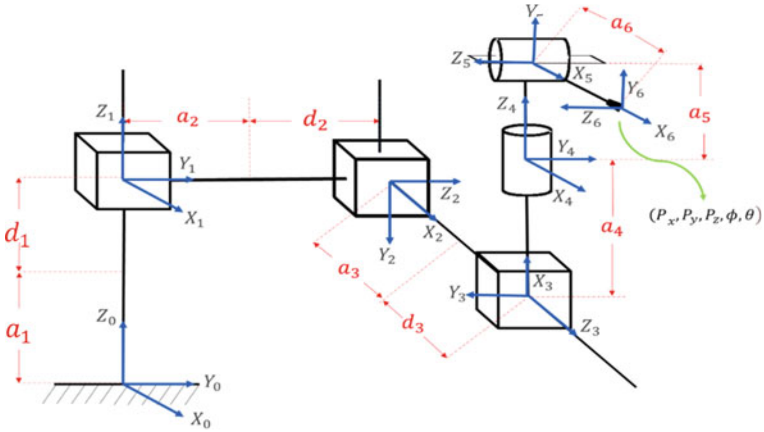

Fig. 13.3 Diagram of the 5 DOF robot for inspection tasks

Table 13.1 Denavit-Hartenberg parameters of the robot

Joint i	θ_i	d_i	a_i	α_i
1	0	d_1	a_1	0
2	0	d_2	a_2	0
3	0	d_3	a_3	0
4	θ_1	0	a_4	0
5	θ_2	0	a_5	0

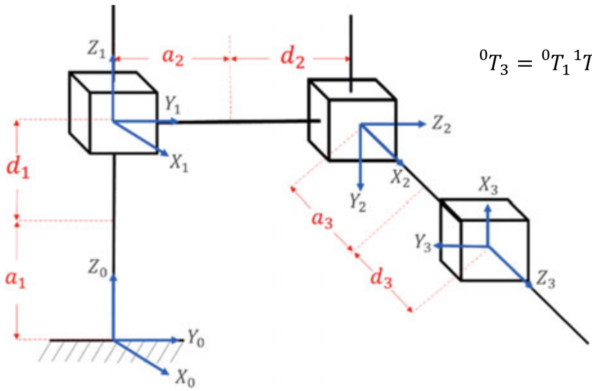

$$ {}^{0}T_3 = {}^{0}T_1\, {}^{1}T_2\, {}^{2}T_3 = \begin{bmatrix} 0 & 0 & 1 & a_3 + d_3 \\ 0 & -1 & 0 & a_2 + d_2 \\ 1 & 0 & 0 & a_1 + d_1 \\ 0 & 0 & 0 & 1 \end{bmatrix} $$

Fig. 13.4 Transformation matrix from frame 0 to frame 3

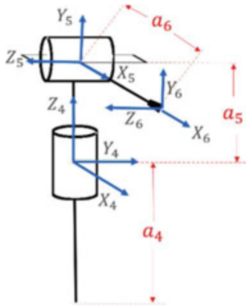

$$^{4}T_6 = {}^{3}T_4\,{}^{4}T_5\,{}^{5}T_6 = \begin{bmatrix} c\theta_1 c\theta_2 & -c\theta_1 s\theta_2 & s\theta_1 & a_6 c\theta_1 c\theta_2 \\ s\theta_1 c\theta_2 & -s\theta_1 s\theta_2 & -c\theta_1 & a_6 s\theta_1 c\theta_2 \\ s\theta_2 & c\theta_2 & 0 & a_4 + a_5 + a_6 s\theta_2 \\ 0 & 0 & 0 & 1 \end{bmatrix}$$

Fig. 13.5 Transformation matrix from frame 4 to frame 6

$$^{0}T_6 = \begin{bmatrix} c\theta_1 c\theta_2 & -c\theta_1 s\theta_2 & s\theta_1 & a_3 + d_3 + a_6 c\theta_1 c\theta_2 \\ s\theta_1 c\theta_2 & -s\theta_1 s\theta_2 & -c\theta_1 & a_2 + d_2 + a_6 s\theta_1 c\theta_2 \\ s\theta_2 & c\theta_2 & 0 & a_1 + d_1 + a_4 + a_5 + a_6 s\theta_2 \\ & 0\ 0\ 0 & & 1 \end{bmatrix} \tag{13.2}$$

In this way, the position P_x, P_y, P_z of the end effector will be given by the last column of the previous matrix:

$$P_x = a_3 + d_3 + a_6 c\theta_1 c\theta_2 \tag{13.3}$$

$$P_y = a_2 + d_2 + a_6 s\theta_1 c\theta_2 \tag{13.4}$$

$$P_z = a_1 + d_1 + a_4 + a_5 + a_6 s\theta_2 \tag{13.5}$$

Finally, with the rotational part $^{0}R_6$ of matrix $^{0}T_6$ it is possible to calculate the Euler angles that define the end effector orientation:

$$R(\psi, \varphi, \theta) = \begin{bmatrix} c\varphi c\theta & s\varphi s\psi c\theta - c\psi s\theta & s\varphi c\psi c\theta + s\psi s\theta \\ c\varphi s\theta & s\varphi s\psi s\theta + c\psi c\theta & s\varphi c\psi s\theta - s\psi c\theta \\ -s\varphi & c\varphi s\psi & c\varphi c\psi \end{bmatrix} \tag{13.6}$$

For the angle φ, matching the element (3, 1) of matrix $^{0}T_6$ with the element (3, 1) of matrix $R(\psi, \varphi, \theta)$:

$$s\theta_2 = -s\varphi \tag{13.7}$$

$$\varphi = -\theta_2 \tag{13.8}$$

For the angle θ, matching the element (2, 1) of matrix ${}^{0}T_{6}$ with the element (2, 1) of matrix $R(\psi, \varphi, \theta)$:

$$s\theta_1 c\theta_2 = c\varphi s\theta \tag{13.9}$$

$$s\theta = \frac{s\theta_1 c\theta_2}{c\varphi} \tag{13.10}$$

Replacing the previously calculated value for the angle φ:

$$s\theta = \frac{s\theta_1 c\theta_2}{c(-\theta_2)} = \frac{s\theta_1 c\theta_2}{c(\theta_2)} = s\theta_1 \tag{13.11}$$

$$\theta = \theta_1 \tag{13.12}$$

From the equations obtained for direct kinematics, the joint variables can be obtained:

$$\theta_1 = \theta \tag{13.13}$$

$$\theta_2 = -\varphi \tag{13.14}$$

$$d_1 = P_z - a_1 - a_4 - a_5 - a_6 s\theta_2 \tag{13.15}$$

$$d_2 = P_y - a_2 - a_6 s\theta_1 c\theta_2 \tag{13.16}$$

$$d_3 = P_x - a_3 - a_6 c\theta_1 c\theta_2 \tag{13.17}$$

13.5 Detailed Robot Design

Based on the design requirements, the detailed CAD design of the robot was performed using AUTOCAD and SKETCHUP software. The design includes: a mobile structure, a mobile platform, a pan-tilt system, and a final effector, Fig. 13.6 shows two views of the final detailed design of the robot that is fully scalable to fit the dimensions of a building's façade.

The mobile structure has wheels, with a braking system, in its four bases for its manual displacement on the ground. Inside, it supports the mobile platform that moves vertically driven by a triple pulleys system mounted at the top of the mobile structure and slides through two vertical rails. The mobile platform moves horizontally through a rack and pinion system, and it moves inward and outward thanks to a

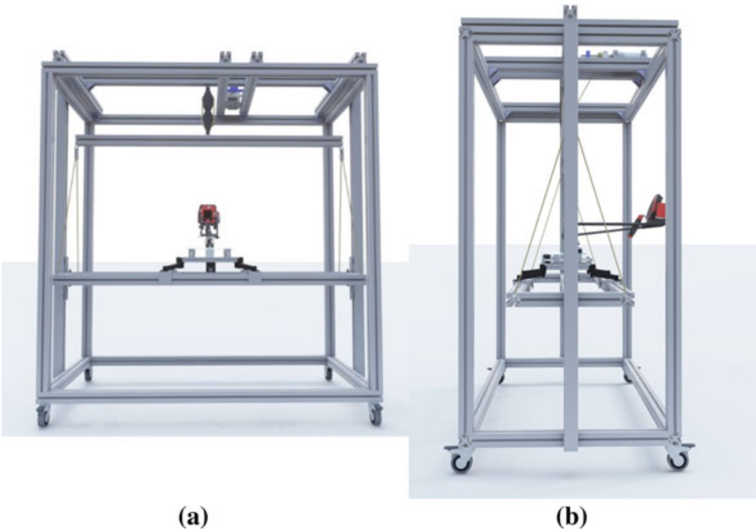

Fig. 13.6 Views **a** frontal and **b** lateral of a scalable prototype proposal

screw-nut transmission. This las motion is very important to adapt to façade profile. Also, the mobile platform supports the pan-tilt system as well as the end effector that holds the pachometer. The Fig. 13.7 shows the main mechanical elements of our proposal to generate the mobility required for an inspection task.

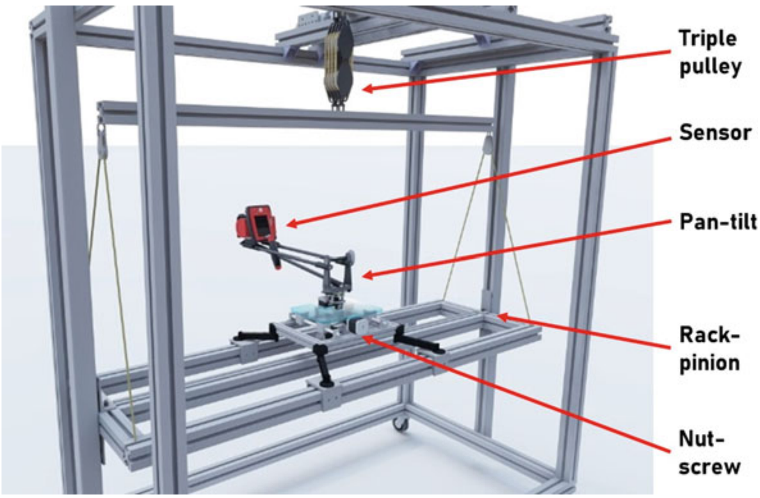

Fig. 13.7 Mechanical elements that generate robot mobility

13.6 Construction of a Laboratory Prototype

To validate the design concept, a laboratory prototype was manufactured. During the process, the following manufacturing requirements were considered: Means to move on the ground, adaptability to the façade profile, zigzag of the end effector, horizontal and vertical maneuverability, simplicity of assembly, weight, and actuators.

The mobile structure of the robot is built in aluminum structural profile with 40 × 40 mm T-groove. At each end of the base of the mobile structure, four 3” rubber wheels are attached, each mounted on a rotating plate with brake. These wheels have thermoplastic properties, polypropylene rims, reinforced bushings, and a load capacity of up to 75 kg each. The mobile platform slides vertically through two iron U-rails and a couple of four-wheel trolley, it is driven by a triple pully with 120 kg capacity and a DC motor. The mobile platform slides horizontally through four 6063T5 aluminum profiles and UHMW antifriction pads, it is driven by a rack and pinion system and a DC motor fixed to the pinion. The rack is made of low carbon steel, type TR with pressure angles of 20°, with an overall length of 1120 mm and a width of 12 mm.

The pan-tilt system, driven by two steppers motors, is mounted on a square acrylic plate, which was mounted to the nut of the screw-nut transmission mechanism which is driven by a DC motor. The square acrylic plate has four legs that were designed and printed in 3D (black color), with a density of 40%. The screw-nut system consists of two 400 mm linear motion rod shaft guides, one 8 mm feed screw, four SK8 shaft supports, four SCS8UU bearings, two KP08 flexible shaft couplings and 2 flexible shaft couplings (Fig. 13.8) .

13.7 Conclusions

This research proposes a 5-DOF for inspection tasks on vertical surfaces. The kinematics are simple since the translations and rotations are all decoupled. The manufactured prototype is light but robust, easy for assembling and enough scalable to adapt to building sizes. Some mobility tests were performed to validate the mechanical assembling. The prototype can perform inspection and some other tasks such as cleaning by changing the sensor with a high-pressure washer. A control system will ensure that the robot follows the zigzag trajectory during an inspection task, a human operator will be able to monitor the task from the ground through a fixed camera mounted on the structure.

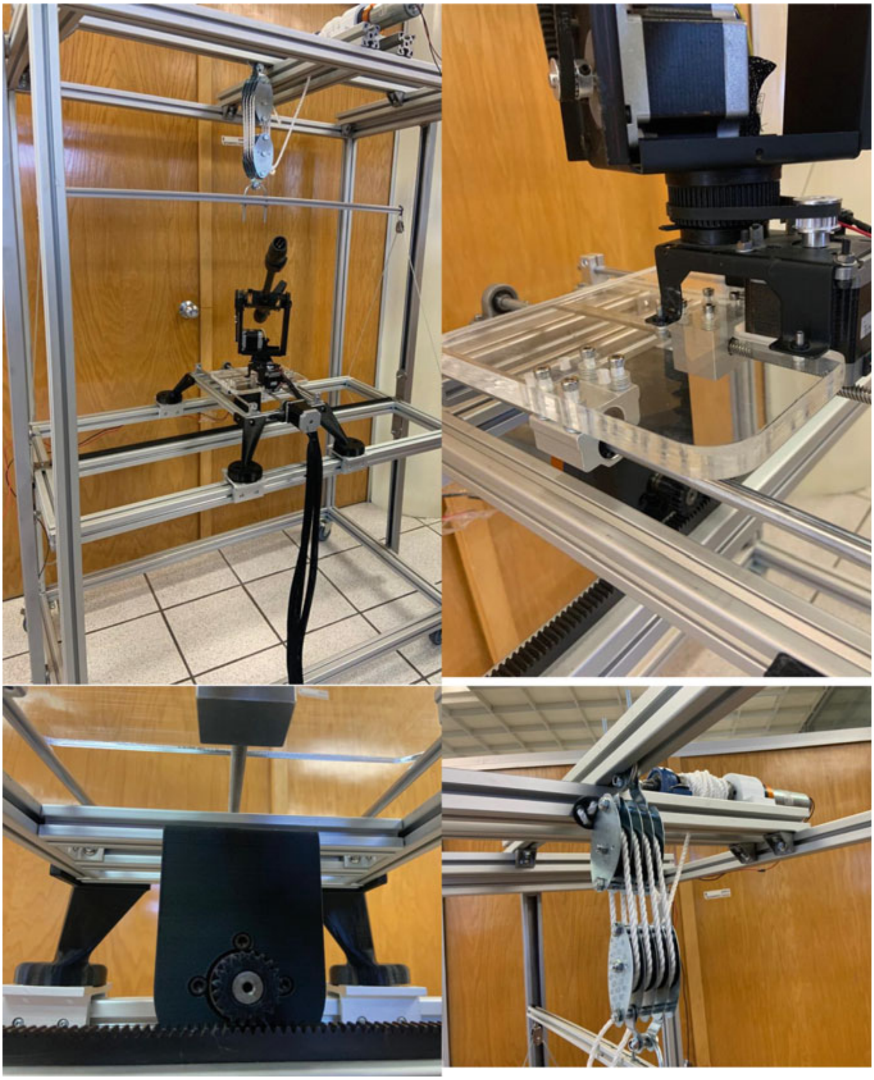

Fig. 13.8 Views of the manufactured prototype

References

1. IFR Press Conference. Frankfurt (2020). https://ifr.org/DOWNLOADS/PRESS2018/PRESENTATION_WR_2020.PDF
2. Riobo, J. et al.: New robotic systems of inspection and intervention in façade rehabilitation (2018). https://www.researchgate.net/publication/327560208_Nuevos_sistemas_roboticos_de_inspeccion_e_intervencion_en_rehabilitacion_de_fachadas_New_robotic_systems_of_inspection_and_intervention_in_facade_rehabilitation

3. Nansai, S., Mohan, R.: A survey of wall climbing robots: recent advances and challenges. Robotics **5**(3). https://doi.org/10.3390/robotics5030014
4. Minmoon, S., Jaemyunghuh, S.D., Soohan, Ch.: Vertical motion control of building façade maintenance robot with built-in guide rail (2015)
5. Kawasaki, S., Kikuchi, K.: Development of a small legged wall climbing robot with passive suction cups. In: Proceedings of the 3rd International Conference on Design Engineering and Science—ICDES, pp. 112–116. Pilsen, Czech Republic (2014)
6. Wang, Y., Liu, S., Xu, D., Zhao, Y., Hao, S., Gao, X.: Development and application of wall-climbing robots. In: Proceedings of the 1999 IEEE International Conference on Robotics and Automation, Vol. 2, pp. 1207–1212. Detroit, AL, USA, 10–15 (1999)
7. Xu, Z., Ma, P.: A wall-climbing robot for labelling scale of oil tank's volume. Robotica **20**, 209–212 (2002)
8. Zhang, H., Zhang, J., Liu, R., Zong, G.: Mechanical design and dynamics of an autonomous climbing robot for elliptic half-shell cleaning. Int. J. Adv. Robot. Syst. **4**, 437–446 (2007)
9. Funatsu, M., Kawasaki, Y., Kawasaki, S., Kikuchi, K.: Development of cm-scale wall climbing hexapod robot with claws. In: Proceedings of the 3rd International Conference on Design Engineering and Science—ICDES, pp. 101–106. Pilsen, Czech Republic (2014)
10. Schmidt, D., Berns, K.: Climbing robots for maintenance and inspections of vertical structures—a survey of design aspects and technologies. Robot. Auton. Syst. **61**, 1288–1305 (2013). https://doi.org/10.1016/j.robot.2013.09.002
11. CMP Express, Periodic facade inspection. https://cmpexpress.com.sg/periodic-facade-inspection/